Redox Biology 58 (2022) 102549

Contents lists available at ScienceDirect

Redox Biology

journal homepage: www.elsevier.com/locate/redox

Specific inhibition of NADPH oxidase 2 modifies chronic epilepsy

Prince Kumar Singh [1], Aseel Saadi [1], Yara Sheeni, Tawfeeq Shekh-Ahmad [*]

The Institute for Drug Research, The School of Pharmacy, Faculty of Medicine, The Hebrew University of Jerusalem, Jerusalem, 91120, Israel

ARTICLE INFO

Keywords:
NOX2
Reactive oxygen species
Temporal lobe epilepsy
gp91ds-tat
Status epilepticus

ABSTRACT

Recent work by us and others has implicated NADPH oxidase (NOX) enzymes as main producers of reactive oxygen species (ROS) following a brain insult such as status epilepticus, contributing to neuronal damage and development of epilepsy. Although several NOX isoforms have been examined in the context of epilepsy, most attention has focused on NOX2. In this present study, we demonstrate the effect of gp91ds-tat, a specific competitive inhibitor of NOX2, in *in vitro* epileptiform activity model as well as in temporal lobe epilepsy (TLE) model in rats. We showed that in *in vitro* seizure model, gp91ds-tat modulated Ca^{2+} oscillation, prevented epileptiform activity-induced ROS generation, mitochondrial depolarization, and neuronal death. Administration of gp91ds-tat 1 h after kainic acid-induced status epilepticus significantly decreased the expression of NOX2, as well as the overall NOX activity in the cortex and the hippocampus. Finally, we showed that upon continuous intracerebroventricular administration to epileptic rats, gp91ds-tat significantly reduced the seizure frequency and the total number of seizures post-treatment compared to the scrambled peptide-treated animals.

The results of the study suggest that NOX2 may have an important effect on modulation of epileptiform activity and has a critical role in mediating seizure-induced NOX activation, ROS generation and oxidative stress in the brain, and thus significantly contributes to development of epilepsy following a brain insult.

1. Introduction

Reactive oxygen species (ROS) are critical intercellular signaling molecules and their level depends on the activity of ROS-producing enzymes and the antioxidant capacity of cells [1,2]. Under physiological conditions, there is a steady balance between ROS generation and the availability of antioxidants [1]. Oxidative stress (OS) arises when the level of ROS overcomes the cellular antioxidant defense, either due to excessive production of ROS or a decrease in cellular antioxidant capacity [1,3]. Accumulating evidence suggests that OS plays a crucial role in acute neurological injuries such as stroke, traumatic brain injuries, and prolonged seizures [3–6] as well as in neurodegenerative disorders such as Alzheimer and Parkinson's diseases [7–9]. Several *in vivo* and *in vitro* studies demonstrated that NADPH Oxidase 2 (NOX2) is a primary source of ROS production, activated by N-methyl-D-aspartate (NMDA) receptors, which leads to neuronal depolarization and increasing of the cytoplasmic Ca^{2+} load, playing an essential role in epileptogenesis and eventually leading to neurodegeneration and cell death [10–14]. Recently, we have demonstrated that following pentylenetetrazol (PTZ) induced seizure, NOX2 expression in the cortex is decreased within 6 h then increased at 24 h post-seizure [15]. Interestingly, we found that in the hippocampus NOX2 was overexpressed for 1–7 days post-seizure. Moreover, we found that NOX2 expression is increased up to 2 weeks following kainic acid induced status epilepticus (SE), in both cortex and hippocampus [15].

Although the engagement of NOX2 with epileptogenesis is well studied, the effect of specific NOX2 inhibition has not been tested yet. Here, we demonstrated that in an *in vitro* epileptiform activity model, selective NOX2 inhibition using gp91ds-tat, suppresses the formation of calcium oscillations, inhibits mitochondrial depolarization, ROS production, and cell death. Moreover, we showed that following kainic acid induced SE, gp91ds-tat decreased the expression of NOX2 and the NOX activity in cortex and hippocampus. Importantly, our studies demonstrate that, selective gp91ds-tat given to chronic epileptic animals results in a significant reduction in the frequency of spontaneous seizures as well as in the cumulative number of seizures experienced per animal post treatment. Taken together, these data indicate that selective NOX2 inhibition represents a novel approach to reduce neuronal death and modify chronic epilepsy.

* Corresponding author. The Institute for Drug Research, The School of Pharmacy, Faculty of Medicine, The Hebrew University of Jerusalem, Jerusalem, 91120, Israel.
E-mail address: Tawfeeq.Shekh-Ahmad@mail.huji.ac.il (T. Shekh-Ahmad).
[1] P.K.S. and A.S. contributed equally to this work.

https://doi.org/10.1016/j.redox.2022.102549
Received 1 September 2022; Received in revised form 29 October 2022; Accepted 21 November 2022
Available online 28 November 2022

Abbreviations

NOX2	NADPH Oxidase 2
ROS	Reactive Oxygen Species
OS	Oxidative Stress
TLE	Temporal Lobe Epilepsy
KA-SE	Kainic acid induced status epilepticus
aCSF	artificial cerebrospinal fluid
ECoG	Electrocorticography

2. Methods and materials

2.1. Primary cortical cell culture and induction of in vitro epileptiform activity

Mixed cortical neurons and glial cell culture were prepared from Sprague-Dawley rat pups (Hebrew University breeding colony, Jerusalem, Israel) of (P0–P1) postnatal stages [16–18] as previously described [19]. In brief, rat's pups were sacrificed by cervical dislocation and brains were collected; followed by isolation of neocortical tissue and quickly submerged in ice-cold HBSS (Ca^{2+}, Mg^{2+}-free, Sigma, H0304). The neocortical tissues were trypsinized using 1% trypsin (Invitrogen) for 6–7 min at 37 °C, then blocking of trypsinization by 20% FBS (Invitrogen) supplemented HBSS media followed by trituration to dissociate the cells. The neuronal cell suspension was seeded on poly--L-lysine (1 mg/mL, Sigma) coated 25 mm rounded coverslips, and culture was maintained in B-27 and 2 mM L-glutamine supplemented Neurobasal® A medium (Invitrogen) at 37 °C under 5% CO_2 humidified atmosphere with CO_2 incubator. Experiments were carried out at 13–17 days *in vitro* (DIV) to allow for full maturation of synapse of cells. Neuronal cell population can be distinguished from glia using phase-contrast microscopy.

In vitro epileptiform activity was induced by omitting magnesium from recording solution *i.e., artificial cerebrospinal fluid (aCSF),* as described previously [20]. For calcium oscillations recording, primary neuronal cells were treated with 0.005% Pluronic acid and 5 mM Fura-2-AM (Thermo Fisher, Invitrogen) in aCSF for 30 min, then cells were washed 3 times.

In vitro low magnesium model or control cells (under aCSF) were pre-incubated for 1 h either with NOX2 specific inhibitor *i.e.,* Gp91 ds-tat, (5 μM) or with Gp91 ds-tat scrambled peptide (5 μM) before performing the subsequent *in vitro* assays.

2.2. In vitro recording solution

All experiments were conducted at room temperature in HEPES buffered salt solution either containing aCSF or excluding $MgCl_2$ (low-Mg^{2+}) to induce an *in vitro* seizure model. Composition of aCSF contains: 125 mM NaCl, 2.5 mM KCl, 2 mM $MgCl_2$, 1.25 mM KH_2PO_4, 2 mM $CaCl_2$, 30 mM glucose and 25 mM HEPES, and pH was adjusted to 7.4 with NaOH.

2.3. Imaging of mitochondrial membrane potential (Δψm)

For measurement of mitochondrial membrane potential (Δψm), Culture coverslip carrying dishes were loaded with 1 M Rhodamine 123 (Rh-123) (Sigma, UK) for 15 min prior to recording, followed by three-time washing. Increased Rh-123 signaling indicates mitochondrial depolarization. Rh-123 signals were normalized to the baseline (set 0), and the maximal signal produced by mitochondrial oxidative phosphorylation uncoupling with carbonylcyanide-*p*-trifluoromethoxyphenyl hydrazone (FCCP, 1 M; set to 100). Each experiment was conducted five to seven times in three independent cultures.

2.4. Imaging of intracellular ROS generation

To measure the rates of reactive oxygen species (ROS) generation in the cytosol, 5 mM dihydroethidium (HEt) was maintained in all solutions throughout the procedures. To prevent the formation of oxidized products, no preincubation was performed. Each experiment was done with three independent cultures and replicated on 5–6 coverslips from each culture.

2.5. Neuronal death assay

Neuronal death was assessed following a 2-h incubation with low-Mg^{2+} at 37 °C, cells were co-stained with 20 μM propidium iodide and 4.5 μM Hoechst-33342 stain (Sigma, St. Louis, MO) in a fluorescent live/dead assay. Experiments were carried out on 3–5 independent cortical cultures and repeated on 5–7 coverslips of each experiment. In each treated culture coverslip, 5–7 random fields were selected for analysis.

2.6. Live imaging and analysis

Fluorescence imaging was performed using a 20 × fluorite objective coupled epifluorescence inverted microscope with xenon arc lamp providing excitation light beam passing at 530 nm (dihydroethidium) (Cairn Research, Kent, UK). Emitted fluorescence was detected by a cooled CCD camera (Retiga; QImaging). Phototoxicity and photobleaching of cells were minimized by limiting light exposure to the time of acquisition of the images. Fluorescent images were captured with a 5 s of a frame interval. Data were analyzed with Andor software (Belfast, UK). HEt was excited by illumination at 530 nm. For most of the experiments, we chose to perform measurements of ROS production rates with dihydroethidium at a single wavelength to avoid photobleaching and phototoxicity from the excitation of cells in the range of UV light. Rates of ROS increase were determined at various time points (2, 10, and 15 min) following exposure to low-Mg^{2+} and were compared with rates recorded during a 1–3 min artificial CSF exposure period referred to as the baseline.

2.7. Quantitative real time - polymerase chain reaction

The NOX2 mRNA level was determined by quantitative RT-PCR using our previously reported primers [15]. Total RNA from cortex and hippocampus were extracted using tri-Reagent (Sigma-Aldrich, St. Louis, MO, USA) and subsequently purity and quantity was determined by Nanodrop spectrophotometry (Nanodrop Technologies, Thermo, Waltham, MA, USA); and ratios of 260:280 were 1.8–2.0. Complementary DNA (cDNA) were synthesized using 1 μg of extracted RNA utilizing oligo-dT15 primers and GoScriptTM reverse transcription system (Promega, Madison, WI, USA). The expression of NOX2 was measured with SYBR Green (PerfeCTa SYBR Green FastMix, Quantabio) and RT-PCR instrument (CFX Bio-rad). Master-mix from each hippocampus and cortex tissue sample were prepared separately with final volume of 15 μl per reaction (7.5 μl SYBER green; 3 μl primers (500 nM each); 3 μl of cDNA template and .5 μl of DEPC water) and subjected to RT-PCR reaction cycle. RT-PCR reaction cycle comprise of initial incubation for 15 min at 95 °C followed by 40 cycles of denaturation of 5 s at 95 °C, 15 s at 60 °C and final step of 5 s at 65 °C and 30 s at 95 °C. For each mRNA, expression of GAPDH (as control) were also analyzed. Each PCR reaction was performed in duplicates and result were calculated and expressed with respected to control and normalized to sham-operated animals, and relative expression of each gene were determined using method described by Pfaffl et al., 2001 [21].

2.8. Estimation of NADPH oxidase activity

The NADPH oxidase activity was determined using the previously described method [22]. Animals were anesthetized deeply using

ketamine (100 mg/kg) and xylazine (10 mg/kg) and their brains were collected immediately, and cortex and hippocampus were recovered. Hippocampus and cortex were homogenized and 20 μl of homogenate of hippocampus and cortex were mixed separately with 900 μl HEPES buffer of pH 7.4 including triethylenetetramine (1.0 mmol/L), L- N (G)-nitro-arginine methyl ester (L-NAME) (1 mmol/L), an inhibitor of nitric oxide synthase (NOS), to determine the enzymatic source of ROS, 20 μM/L lucigenin, and SDS (100 μM/L) and aliquot into 96-well under dark condition at room temperature. Basal luminescence was monitored using luminometer and enzymatic activity was triggered by adding 0.2 mmol/L of NADPH and enzymatic activity were recorded for 15 min. Blank reading were subtracted from tissue homogenate-added wells. The chemiluminescence changes per minute per mg protein in hippocampus and cortex were determined for percentage change versus sham operated animals.

2.9. Kainic acid-induced status epilepticus

Status epilepticus (SE) was induced using kainic acid (KA) administered according to a previously described protocol (Hellier et al., 1998) [23]. Briefly, adult male and female Sprague Dawley rats (weight, 200–250 g) were injected intraperitoneally with KA (Hello Bio, Bristol, UK) dissolved in sterile 0.9% saline (10 mg/ml). Injections were administered hourly at a dose of 5 mg/kg until class III, IV, or V seizures were evoked (scored according to a modified Racine's scale (Racine, 1972; Ben-Ari, 1985)) [24,25]. KA administration was halted when animals reached class V seizures (rearing with forelimb clonus and falling over) or when the total dose of KA reached 45 mg/kg. Animals were included in the study if there was continuous motor seizure activity for 2 h following the final dose of KA. Ten to 12 weeks after the induction of SE, rats were implanted with ECoG transmitters to allow for wireless telemetry recordings, and a brain infusion cannula to access the lateral ventricle.

2.10. Surgical procedures

Animal experiments were conducted in accordance with the Association for Assessment and Accreditation of Laboratory Animal Care International and approved by the Institutional Animal Care and Use Committee of the Hebrew University of Jerusalem (Approve number: MD-20-16254-5). Naïve male and female Sprague–Dawley rats (180–220 g), a strain of the Hebrew University (obtained from Harlan, Jerusalem, Israel) were housed under controlled environmental conditions (23C; 50–60% humidity; 12-h light/dark cycle) with free access to food and water. Animals were acclimatized for 7 days prior to experimental use.

Rats (200–250 g) were anesthetized using isoflurane (3% induction, 1.5–2% for surgery) and fixed to the stereotaxic frame (Kopf, CA, USA). Before initiating the surgery, rats were injected with buprenorphine (0.2 mg/kg; SC) and Metacam (1 mg/kg; SC) for pain relief. An ECoG transmitter (A3028E, Open-Source Instruments) was implanted subcutaneously with two subdural intracranial electrodes. The recording electrode was positioned above the right hippocampus [2.5 mm lateral and 4 mm posterior of bregma (Paxinos and Watson, 2014)] [26], and a reference electrode was implanted in the contralateral hemisphere (2.5 mm lateral and 6 mm posterior of bregma (Paxinos and Watson, 2014) [26]. The electrodes were fixed to the skull with three skull screws and tissue glue. A brain infusion cannula (Brain Infusion Kit 2, Alzet) connected to vinyl catheter tube was implanted into the right lateral ventricle of brain [1 mm posterior, 1.2 mm lateral, 4.5 mm ventral from the bregma, Paxinos and Watson, 2014)]. The catheter tube was plugged (to allow later connection to mini osmotic pump) and a tunnel was created to place the tube into a subcutaneous cavity. At the end of surgery, brain incision was sealed with dental cement and rats were injected with 3–5 ml of warmed Ringer's solution and amoxicillin (Betamox LA, 100 mg/kg).

For the infusion of gp91ds-tat and scrambled peptide, following 3 weeks of baseline ECoG recording, epileptic rats were randomly assigned to one of two groups, either gp91ds-tat or its scrambled peptide. Rats were anesthetized with isoflurane (2.5%) and then subjected to stereotaxic implantation of mini osmotic pump (Alzet, model 2002). The pump was connected to the previously implanted vinyl catheter tube for ICV infusion of gp91ds-tat or its scrambled peptide as a control (800 ng/kg/day, 0.5 μl/h) for 2 weeks.

2.11. Statistical analysis

Statistical analyses were performed with GraphPad Prism v9.3.1 (GraphPad software, USA). Data acquisition and analysis were done blindly. All quantitative data represented as mean ± standard error of mean (mean ± SEM), where n indicates number of individual samples. Unpaired Student's *t*-test, ordinary one-way analysis of variance (ANOVA) with Tukey's post hoc test, or two-way ANOVA with Dunnett's post hoc test were used for data analysis as appropriate. The effects of treatment on normalized seizure frequency (Fig. 4C were analyzed using a generalized log-linear mixed model with random effect of animal (autoregressive covariance) and fixed effects of treatment group, week, and the interaction between treatment group and week. Statistical significance was defined as a value of $p < 0.05$ and $p < 0.01$. Sample sizes were determined based on previous experience with calculating experimental variability. The number of animals utilized are specified in the respect figures.

3. Results

3.1. Gp91ds-tat alters Ca^{2+} oscillation during epileptiform activity

Using an *in vitro* Ca^{2+} oscillation assay of epilepsy [27], we first tested whether selective NOX2 inhibition by gp91ds-tat can modulate epileptiform network activity. We induced epileptiform activity in the rat mixed cortico-culture by omitting Mg^{2+} from culturing medium, which promote activation of NMDA receptor through release of vesicular glutamate resulting in epileptiform activity and Ca^{2+} oscillations in neurons [28]. The removal of Mg^{2+} from the culturing media induces synchronized Ca^{2+} signaling in the untreated neuronal culture (Fig. 1A). Interestingly, when cultures were treated with gp91ds-tat (5 μM), we observed a reversible inhibition of Ca^{2+} oscillations that were restored after washing out the gp91ds-tat (Fig. 1A). During washing in the gp91ds-tat ($n = 7$), the Ca^{2+} frequency decreased from 2.9 peaks/minute to 0.6 peaks/minute (Fig. 1B, $p < 0.0001$ One-way ANOVA with Tukey post-hoc test). In addition, the amplitude of Ca^{2+} peaks was also decreased by ~4 fold (from 1.9 to 0.5; Fig. 1C; $p < 0.0001$). Importantly, both the frequency and the amplitude of Ca^{2+} peaks were restored to baseline levels following wash out of gp91ds-tat (Fig. 1B–C).

Notably, cultures treated with scrambled peptide (scrm gp91ds-tat) had no difference neither in frequency nor in amplitude of Ca^{2+} peaks (Fig. 1D–E). These data indicates that selective inhibition of NOX2 isoform with gp91ds-tat alter either vesicular glutamate release or activation of NMDA receptor in low Mg^{2+} model of *in vitro* epileptiform activity.

3.2. NOX2 inhibition prevents mitochondrial depolarization and promotes neuroprotection

A low level of mitochondrial substrates or the opening of the mitochondrial permeability transition pore may be the causes of mitochondrial depolarization that results from prolonged seizure-like activity in neurons [28,29]. Omitting Mg^{2+} from the recording solution induced slow and progressive mitochondrial depolarization in neuronal culture resulting in 30% reduction in mitochondrial membrane potential ($\Delta\psi m$) following 30 min (Fig. 2A). Pre-treatment of neuronal cultures with gp91ds-tat (5 μM-1 hr of preincubation, $n = 5$) prevented the

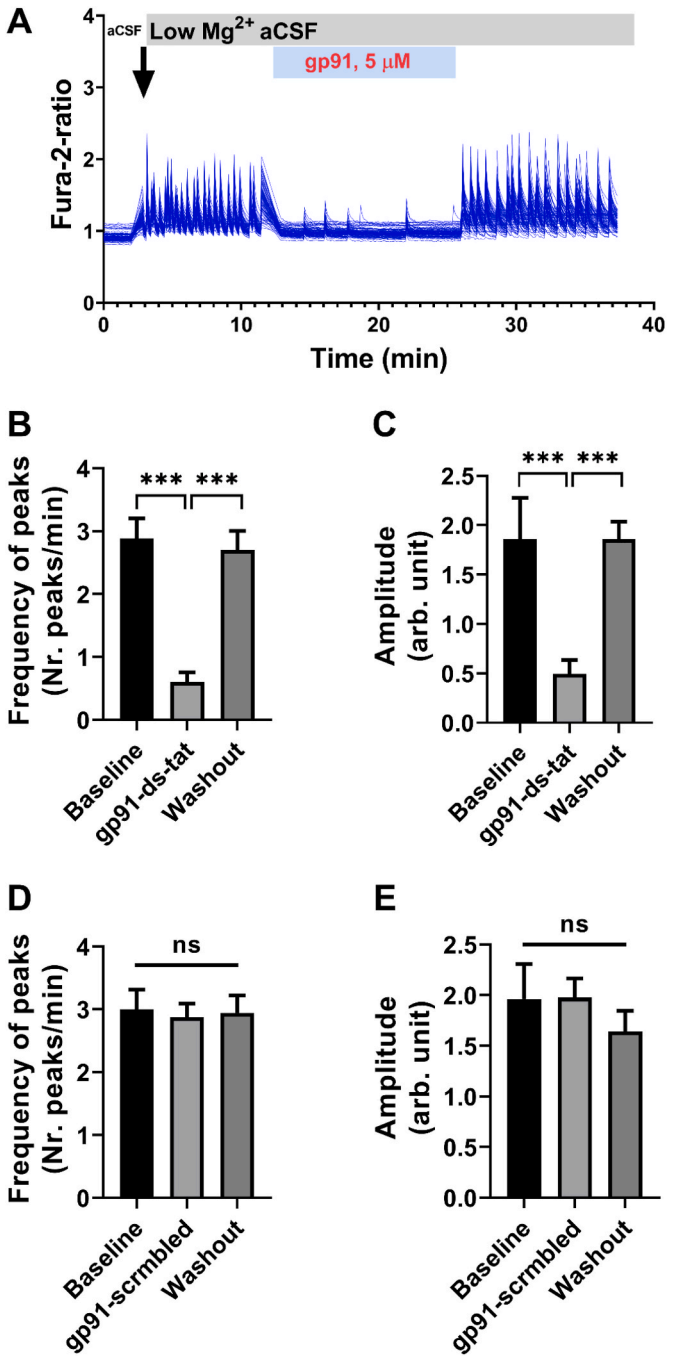

Fig. 1. Gp91 ds-tat modulated Ca^{2+} oscillatory signal in neurons.
(A) Representative image of synchronous Ca^{2+} oscillatory signal in neurons, indicating epileptiform activity induced by replacement of artificial CSF (aCSF) with low Mg2+ aCSF (indicated by arrow) before, during and after washout of gp91 (5 μM) to the coverslip solution. (B–C) Bar graphs summarizing the effect of gp91 (5 μM) on frequency (B) and the amplitude of Ca^{2+} oscillations recorded from rat neuronal cultures (n = 7 experiments) at 13–17 DIV. (D–E) Bar graphs summarizing the effect of scrambled gp91 ds-tat (control; 5 μM) on frequency (D) and the amplitude of Ca^{2+} oscillations (n = 7 experiments). Data are expressed as mean ± SEM. ***P < 0.001 relative to low-Mg^{2+} condition, by one-way ANOVA with Tukey's post hoc test. ns = not significant.

epileptiform activity-induced mitochondrial membrane potential (Δψm) depolarization (Fig. 2A). Consistent with previous reports [11, 30] we found that low Mg^{2+} induced epileptiform activity increases the rate of ROS production up to 5-fold (n = 5, Fig. 2B). Upon selective inhibition of NOX2 with gp91ds-tat (5 μM-1 hr of preincubation), the

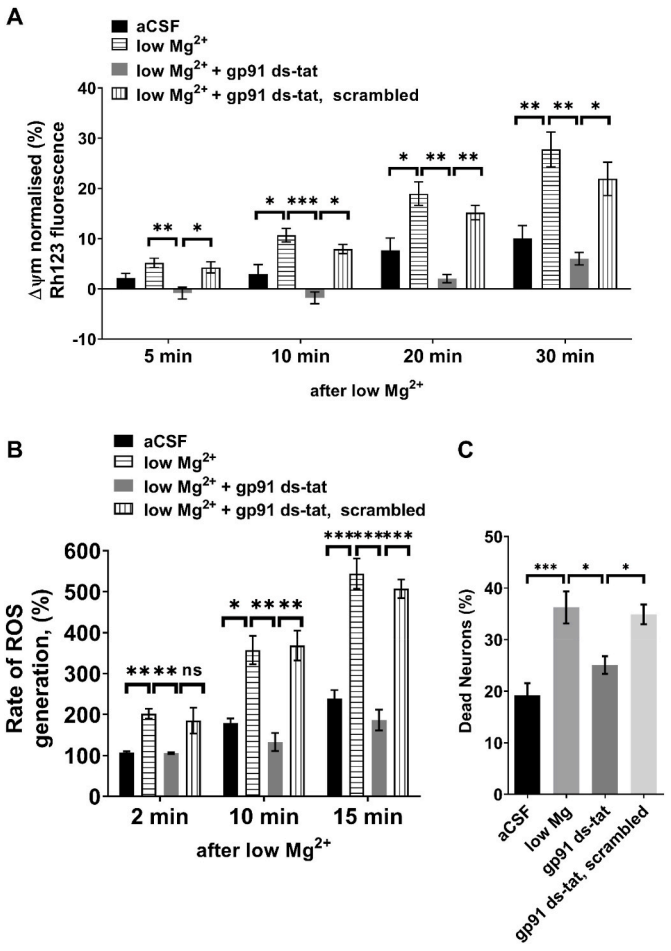

Fig. 2. Selective inhibition of NOX2 promotes neuroprotection *in-vitro*.
(A) Normalized Rh-123 fluorescence of neurons 5, 10, 20 and 30 min stimulated with either aCSF (n = 6 experiments (exp.), or low Mg^{2+} (n = 6 exp.) and treated acutely either with gp91ds-tat peptide (5 μM; n = 6 exp.) or with scrambled peptide (5 μM). (B) Normalized rates of ROS generation in neurons at 2, 10, and 15 min in aCSF, low Mg^{2+} aCSF, and gp91ds-tat (5 μM) or scrambled peptide-treated neurons in low-Mg^{2+} condition (n = 5 exp for all groups). (C) The percentage of neuronal cell death in cultures following 2 h exposure to aCSF (n = 7), low Mg^{2+} (n = 7), and treatment with either gp91ds-tat (5 μM; n = 7 exp.) or with scrambled peptide (5 μM). Data (Mean ± S.E.M.) were analyzed by either Two-way ANOVA followed by Dunnett's post hoc test (A and B) or one-way ANOVA (C) followed by Tukey's post hoc test. *P < 0.05, **P < 0.01 and ***P < 0.001 versus low Mg^{2+} condition.

rate of ROS production was significantly reduced during epileptiform activity from 202% to 106%, 2 min post exposure to low-Mg2+ (Fig. 2B, p = 0.039); and from 357% to 133% and 544%–186% at 10-, and 15-min post exposure to low-Mg^{2+}, respectively (Fig. 2B; p < 0.0001). In agreement with previous reports, we found that epileptiform activity induced by low Mg^{2+} (for 2 h) is associated with increased neuronal cell death compared with artificial CSF (36% vs. 19%, p < 0.0001; Fig. 2C). We therefore asked whether the effect of selective NOX2 inhibition using gp91ds-tat on mitochondrial membrane potential and ROS production translated to a neuroprotective effect. Pre-treatment of neuronal cultures with gp91ds-tat (5 μM, 1 h) significantly rescued neurons from epileptiform activity-induced cell death (Fig. 2C, p = 0.012 vs. low Mg^{2+}).

3.3. Gp91ds-tat reduces NOX2 expression and NOX activity following KA-SE

To determine the effect of gp91ds-tat on NOX2 expression and NOX

activity *in-vivo*, we analyzed brain samples at a time when NOX2 expression peaked in hippocampus of rats after status epilepticus (SE), i.e., 24 h post-SE [15]. Rats were first injected with kainic acid to induce SE. After 2 h of SE, rats were injected with diazepam (10 mg/kg, *i. p.*) then 1 h later followed by intracerebroventricular (ICV) administration of 400 ng/kg gp91ds-tat (Fig. 3A). Treatment with gp91ds-tat at 1 h after SE significantly reduced the up-regulation of the SE-induced NOX2 expression in the cortex and in the hippocampus (Fig. 3B–C; SE-vehicle vs. SE-gp91 ds-tat, cortex: $p = 0.0329$; hippocampus: $p = 0.005$).

We further investigated the effect of gp91ds-tat treatment on overall NOX enzyme activity in the cortex and hippocampus of rats following SE. We found that gp91ds-tat significantly inhibited the NOX catalytic activity by 55% and 60% in the cortex and the hippocampus, respectively (Fig. 3D–E; SE-vehicle vs. SE-gp91 ds-tat, cortex: $p = 0.01$; hippocampus: $p = 0.007$).

Moreover, along with the NOX activity in the cortex, we observed a

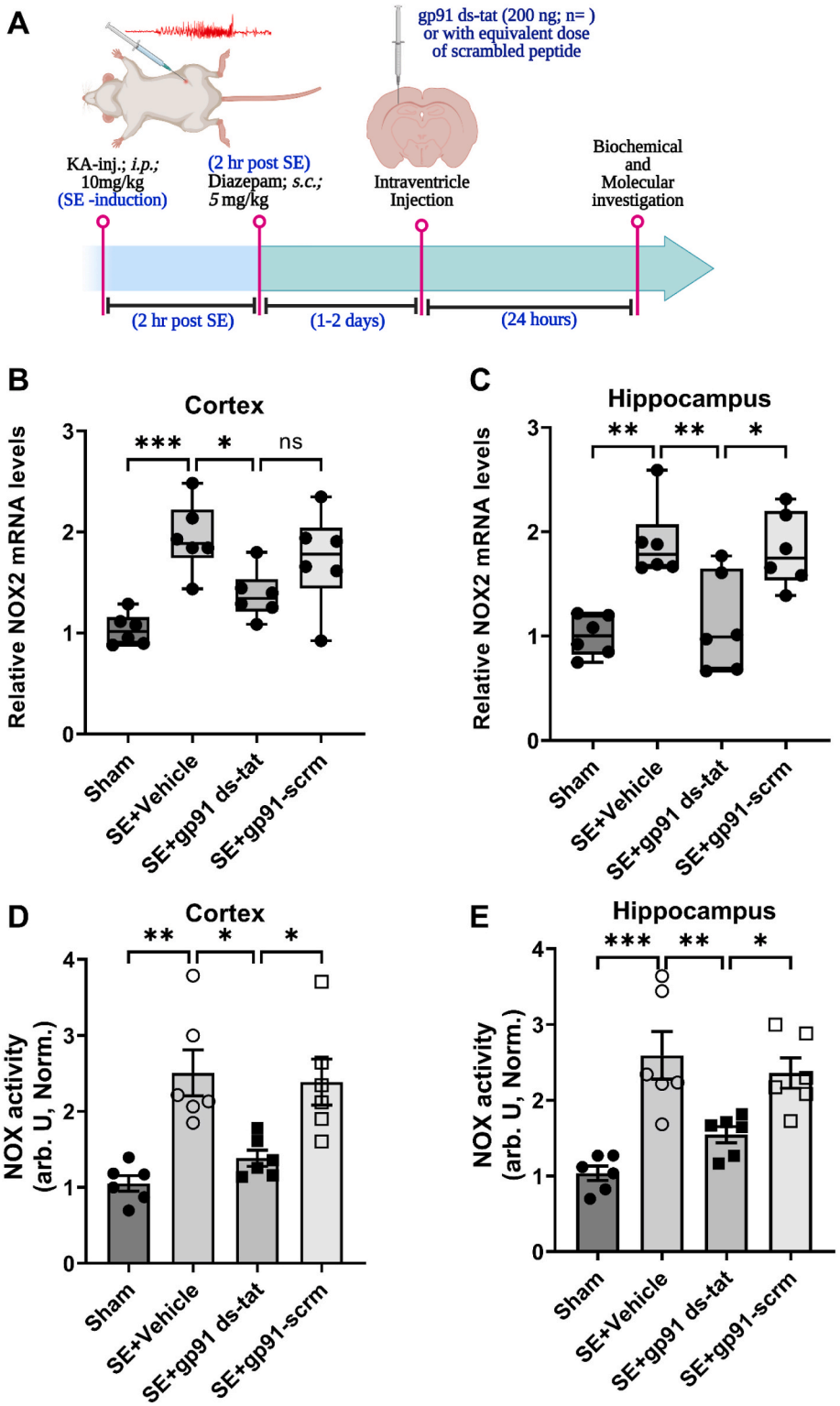

Fig. 3. Gp91 ds-tat suppresses mRNA expression of NOX2 and inhibits the NOX activity in the brain following SE.
(A) Schematic diagram of experimental design and procedures to determine the NOX2 mRNA expression and NOX activity in the study. (B–C) NOX2 mRNA expression in the cortex (B, $n = 6$) and the hippocampus (C, $n = 6$) of gp91ds-tat (400 ng/kg) or its scrambled peptide treated rats following SE (relative to sham group). (D–E) Normalized NOX activity in the cortex (D; $n = 6$) and the hippocampus (E, $n = 6$) of gp91ds-tat (or its scrambled peptide) treated rats following SE (relative to sham group). Data are expressed as mean ± SEM. $^{*}P < 0.05$, $^{**}P < 0.01$ and $^{***}P < 0.001$ versus kainic acid group, by one-way ANOVA with Bonferroni post hoc test.

similar pattern of ROS production. We found that the increase in NOX activity in the cortex of rats after SE was accompanied by a significant (~3-fold) increase in ROS production, which was significantly reduced by treatment with gp91ds-tat (Supplementary Fig. 1).

3.4. NOX2 inhibition modifies chronic epilepsy

Next, we investigated the alleviating effect of gp91ds-tat treatment on chronic epilepsy. To this end, we performed a randomized trial in a rat model of temporal lobe epilepsy (TLE) induced by systemic KA injection. Ten to twelve weeks after induction of SE, rats were implanted with wireless electrocorticography (ECoG) transmitters for monitoring the development of spontaneous seizures. We first performed a baseline ECoG recording for 3-weeks. Epileptic animals were then randomized to treatment with either gp91ds-tat or its scrambled peptide control (n = 9 rats/group), given via ICV administration over 2-weeks using osmotic pumps. ECoG recording was continued during the 2 weeks treatment period and for additional 8 weeks. Treatment with gp91ds-tat significantly decreased the normalized (to baseline) seizure frequency compared to scrambled peptide following treatment (generalized log-linear mixed model on week's 1–10, treatment group*week interaction effect: $F(13,208) = 5.138$, $P < 0.001$; Fig. 4C). Moreover, the normalized cumulative number of seizures post treatment was significantly reduced in the gp91ds-tat group compared to the scrambled peptide group (Fig. 4C–D, $P = 0.026$ Student's t-test). Altogether, these findings suggest that targeting NOX2 with a specific peptide inhibitor gp91ds-tat has a modifying effect on chronic epilepsy.

4. Discussion and conclusion

Accumulating evidence suggested that oxidative stress and overproduction of ROS play a crucial role in epilepsy. Under oxidative stress, it stimulates cascade of events responsible for epileptogenesis [3]. During this seizure-free latent phase, a series of neurological alterations like neuroinflammation, neurodegeneration and aberrant neuroregeneration and reduction in seizure threshold occurs, which eventually leads to spontaneous recurring seizures [3]. In the last decade, the ROS-producing enzymes NADPH Oxidases (NOX) attracted great research interest in its contribution to the ROS burden as well as in its functional role in various neurological diseases including epilepsy. Among the seven NOX isoforms, NOX2 was reported as the main isoform in brain tissues such as glia and neurons [31–33], and its activation has been linked to brain pathology, implying that NOX2-mediated ROS production participates in acute and chronic neurological disease [14,34,35]. Recently, we studied the spatial and temporal expression of NOX2 following the acute seizure model (induced by pentylenetetrazol) and following status epilepticus (SE) induced by systemic administration of kainic acid [15]. We demonstrated that NOX2 has a transient expression pattern in the cortex while in the hippocampus its expression was persistent for up to 1-week post-seizure [15]. Importantly, NOX2 expression was increased up to 2 weeks post-SE, in both the cortex and the hippocampus [15].

Several other researchers have investigated the effect of pharmacological NOX inhibitors on seizure and epilepsy models [10,12,19,36–38]. However, a selective peptide inhibitor of NOX was never tested before in epilepsy. We have previously reported that a pharmacological inhibitor of NOX (i.e., AEBSF) showed no effect on Ca^{2+} oscillations at the tested concentrations in in vitro epileptiform activity model [19]. It remains unclear whether other pharmacological inhibitors of NOX affect the Ca^{2+} oscillations, or whether the effect that we observed with gp91 is a specific feature of this peptide inhibitor. Interestingly, a study by Malkov et al. [37] tested the anti-seizure effect of three pharmacological inhibitors: (2R)-amino-5-phosphonopentanoate (APV), celastrol, and GSK2795039, and found that all three inhibitors strongly reduced seizure activity. The signaling pathway linking the NMDA receptor to NOX involves Ca^{2+} influx which is normally required to induce excitotoxicity, as well as phosphoinositol-3-kinase, and protein kinase C [39,40]. Thus, interventions at any of these steps can prevent ROS production and excitotoxic injury that may explain the observed anti-seizure effects. Nevertheless, future studies are needed to elucidate the exact mechanism by which these NOX inhibitors can modulate seizure activity."

Due to lack of selective pharmacological NOX2 inhibitors, we utilized previously reported peptide-based NOX2-specific inhibitor, gp91 ds-tat, [41] to investigate the effect of specific NOX2 inhibition on *in vitro* epileptiform activity, and on temporal lobe epilepsy rat model. A major advantage of utilizing such peptide-based inhibitors is that they may efficiently block the targeted protein–protein interactions within the enzyme complex important for NOX activity and thus, uniquely block only those sites that are involved in the assembly of the active complex. To date, the available pharmacological NOX inhibitors display a lack of specificity for a single NOX isoform [42]. Gp91 ds-tat is the only isoform-specific peptide-based NOX2 inhibitor currently available [42] that binds to $p47^{phox}$ and inhibits its interaction with $gp91^{phox}$ which blocks the active activation of NOX2 complex and production of superoxide radicals [42–44]. In recent year, Gp91 ds-tat has been widely utilized in various studies to investigate the crucial role of NOX2 in various disease pathophysiology like diabetes [45], hypertension [46],

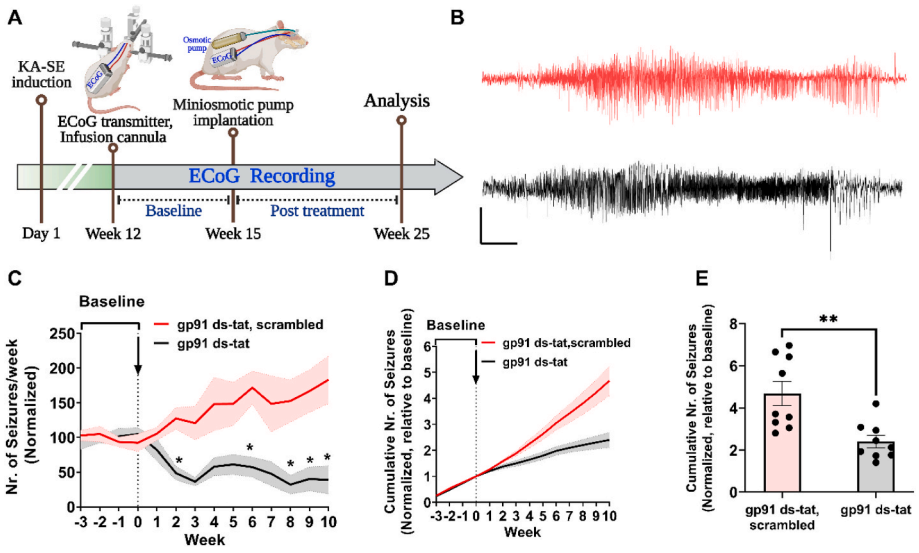

Fig. 4. Selective therapy with gp91ds-tat inhibits seizure progression and modifies chronic epilepsy. (A) Schematic illustration of experimental setup and timeline. (B) Representative seizures from animals subjected to KA-SE and treated with gp91ds-tat (black) or its scrambled peptide control (red). Scale bar: 10 s and 0.5 mV. (C). Normalized seizure frequency (per week, mean ± SEM) in animals recorded for 3-weeks of baseline, then treated (indicated with arrow) either gp91 ds-tat (800 ng/kg/day for 2 weeks; n = 9) or gp91ds-tat scrambled peptide (800 ng/kg/day for 2 weeks; n = 9). (D) Normalized (to baseline) cumulative number of seizures of animals in C. (E) Total number of seizures after treatment, normalized to baseline (pre-treatment). In C: *P < 0.05, by generalized log-linear mixed model followed by Sidak's post hoc test. In E: **P < 0.01, Student's *t*-test). . (For interpretation of the references to colour in this figure legend, the reader is referred to the Web version of this article.)

aging [47], seizure-like activity [11] and Alzheimer's disease [48]. Several investigations demonstrated and reported the high efficacy and specificity of gp91 ds-tat inhibitor to inhibit the NOX2 mediated ROS production in *in vitro* and *in vivo* [44,49,50] and also prevent number of ROS stimulated cascade of events like hypoxia [51], nutrient deprivation [52], endothelin-1 [53], angiopoietin-1 [54], phenylephrine [55], shear stress [56], and so on. Previous studies also showed that gp91 ds-tat efficiently prevents the collagen-induced NOX2 activity in platelets [57] and angiotensin II (AngII)-mediated superoxide production human resistance artery smooth muscle cells [58]. Recent report from Kovac et al. (2014) showed that low Mg^{2+} induced-epileptiform activity resulted in elevated ROS production and Ca^{2+} oscillation activity mediated by NMDA receptor dependent NOX2 activation [11,28]. Our results show that following *in vitro* low Mg^{2+} induced epileptiform activity, selective inhibition of NOX2 using gp91 ds-tat significantly reduce the Ca^{2+} oscillation, a marker of epileptiform activity, as revealed from the immediate decrease in peak's frequency and amplitude (Fig. 1). Interestingly, previous reports showed that Ca^{2+} release from ER specifically regulated by ryanodine receptor (RyR) requires basal NOX2 activity in neuronal and muscle cells [31,59–61] and stimulation of RyR activates Rac1 [62], a subunit of NOX2 complex [63]. Wilson et al., 2016 also demonstrated that inhibition of NOX2 using gp91 ds-tat peptide inhibits the RyR-mediated Ca^{2+} release following stimulation of RyR-mediated Ca^{2+} by 4-CMC (4-chloro-m-cresol) [64]. This reduced Ca^{2+} oscillation was rescued in gp91ds-tat treated cells after removing NOX2 inhibitor *i.e.,* washout condition (Fig. 1A–C). The Ca^{2+} signal was previously characterized for its sensitivity to modulation of four crucial targets of antiepileptic drugs including GABA receptor, glutamate receptor, voltage-gated sodium, and calcium channels [27]. Here, our experiments do not confirm any pinpoint mechanism behind the possible antiepileptic effect of gp91 ds-tat. Rather, we speculate the possibilities based on previous reports on the crosstalk between epileptic ROS and seizure-like activity where specific inhibition of NOX2 using gp91 ds-tat, might have both characteristics of inhibition of NOX2-mediated ROS production and associated neuronal cell death, and possibly, modulation of the vesicular glutamate release or NMDA receptor activation in the low Mg^{2+} model of seizure-like activity. Previous reports showed that following the prolonged seizure like SE, the elevated level of ROS production mediated by NMDA receptor dependent NOX2 activation [11,30]. ROS and the resulting peroxynitrite formation can induce lipid peroxidation, mitochondrial depolarization (mitochondrial permeability transition pore opening), enzyme inactivation, DNA damage and leads to cell death [65]. Similar to previous report [19], our results show that inhibition of NOX2, prevents the epileptiform activity induced mitochondrial membrane depolarization, reduced the ROS production, and prevented the epileptiform activity-induced neuronal cell death (Fig. 2C). However, in our study we used a specific NOX2 inhibitor, isolating, for the first time, the effect of NOX2 isoform on these parameters. Altogether, the neuroprotective effect of gp91ds-tat highlights the profound role that NOX2 isoform plays in seizure-induced cell damage (Figs. 1–2). We further demonstrate the potential of gp91ds-tat to inhibit NOX2 expression and activity *in-vivo*. Indeed, our results demonstrated that gp91ds-tat suppresses the SE-induced overexpression of NOX2, and the increase in overall NOX activity in cortex and hippocampus (Fig. 3). Upon administration of intraventricular injection of NOX2 inhibitor, gp91 ds-tat, to KA-SE rats, prolonged seizure induced overall NOX activity (*i.e.,* SE + Vehicle, Fig. 3D–E) reduced significantly, possibly suggesting that among the 5 major NOX isoforms (i.e., NOX1 to NOX5), NOX2 expression and activity predominantly elevated following prolonged seizure (e.g., KA induced SE). Importantly, we have reported that following KA-induced SE, NOX2 expression is increased in both neurons and astrocytes in the cortex, while in the hippocampus it was increased only in neurons but not in the astrocytes [15].

In fact, many studies have previously shown that non-specific inhibition of NOX can reduce oxidative stress, leading to improved outcomes in seizure and epilepsy models [12,38,66,67]. To the best of our knowledge, we are the first to investigate the therapeutic effect of a specific competitive NOX2 inhibitor in chronic epilepsy model. We employed a well-established model of TLE, *i.e.,* the systemic kainic acid-induced SE [68,69]. In this model, rats are subjected to 2 h of SE (induced by kainic acid injection) that is terminated by diazepam. According to our and others previous reports, spontaneous unprovoked seizures occur within 2-weeks post SE, and progressively increased over time [20,69]. At 10–12 weeks post-SE, these animals reach a chronic epilepsy stage, and the seizure frequency reach a plateau. At this time, epileptic rats were treated (in a randomized and blinded manner) with either gp91ds-tat or its scrambled peptide. We used mini osmotic pumps for continuous intraventricular administration of the peptides directly into the lateral ventricles for a period of 2 weeks. Our results showed that selective NOX2 inhibition via gp91ds-tat in epileptic animals significantly decreased the number of subsequent seizures in comparison to scrambled peptide-treated animals, as was the cumulative number of seizures normalized to baseline (Fig. 4B).

Inflammation appears to play a determinant role in epileptogenesis as well as in chronic epilepsy. In fact, neuroinflammation and oxidative stress are prevalent across many epilepsies, and both are argued to be causal and consequential to the pathogenesis of the disease [70,71]. Among the NOX isoforms, NOX2 has been particularly related to neuronal damage and death, as well as to the resolution of the subsequent inflammatory response after brain injury including SE [72]. It is argued that besides being the major contributor to SE-induced ROS production in acquired epilepsies, NOX2, expressed mainly in microglia, is thought to be the major contributor to the neuroinflammation response [73]. In agreement with these data, we demonstrated that NOX2 was also expressed in the cortex, as well as in CA1 and CA3 of the hippocampus 1 week after SE (Supplementary Fig. 2). The contribution of gp91 to the possible anti-inflammatory effect remains to be elucidated in future studies.

Altogether, our findings demonstrate that specific inhibition of NOX2 reduces the seizure mediated ROS production and showed neuroprotective effect in seizure induced neuronal death in *in vitro* model of epileptiform activity (Fig. 2). Moreover, our results also demonstrated the disease modifying potential of a specific competitive NOX2 peptide inhibitor, gp91ds-tat, in *in vivo* TLE model by reducing the seizure frequency and also the cumulative number of seizures experience by each rat after treatment (Fig. 4). Studies have verified that NOX2 mediated ROS production is related to epilepsy [19,35,37,74–77], suggesting NOX2 as a promising therapeutic target for the prevention and/or modifying epilepsy. The synthetic peptide gp91ds-tat was reported to be an efficacious and specific inhibitor of NOX2 that binds directly to the enzyme, impairing its activity and thus inhibiting ROS production [41]. Despite efficacy in animal models [49,78], gp91ds-tat is very limited by its pharmacokinetic properties, including weak oral bioavailability [79]. It is also not clear whether it can pass the blood-brain-barrier (BBB). Therefore, it is unlikely to be orally active or display a suitable pharmacokinetic profile to have widespread utility as a clinical drug. We, therefore, administered this synthetic peptide via ICV administration. The main limitation of our study is that gp91ds-tat was administered ICV via mini osmotic pumps, which holds little translational value. In spite of that, our study reveals the proof-of-concept that specific inhibition of NOX2 has disease modifying effect on chronic epilepsy. To date, there is only limited knowledge on the role of NOX enzymes on excitability of neurons. Interestingly, our *in vitro* results suggest, for the first time, that NOX2 enzyme may play a vital role in neuronal firing and hyperexcitability.

In conclusion, the current study provides evidence of an important role of NOX2 in epilepsy, not only as ROS producer, but also suggesting anti-epileptic mechanism, and thereby contributes significantly to neuronal death following brain insult such as SE, and to supress the development of seizures. Nevertheless, further studies are needed to investigate the exact mechanism and molecular target of NOX2

responsible for the epileptiform activity modulation.

Funding

This research was supported by The Israel Science Foundation (grant no. 1976/20 to TSA).

Author contributions

PKS: Investigation, Data analysis, Graphical designing, Writing-original draft, reviewing and editing; AS: Investigation, Data analysis, Reviewing and Editing; YS: Investigation; TSA: Conceptualization, Formal data analysis, Writing-original draft, Funding acquisition, and Supervision.

All authors read this manuscript and approved it for publication.

Institutional review board statement

Animal experiments were conducted in accordance with the Association for Assessment and Accreditation of Laboratory Animal Care International and approved by the Institutional Animal Care and Use Committee of the Hebrew University of Jerusalem (protocol code MD-20-16254-5 and date of approval 13 July 2020).

Declaration of competing interest

All authors declared that they have no competing interest in connection with this manuscript.

Data availability

Data will be made available on request.

Acknowledgments

The authors are thankful to The Neubauer Family Foundation for their generous support in our research.

We also acknowledge the David R. Bloom Center for Pharmacy for financial support.

We thank Kevan Hashemi for technical advice with the ECoG telemetry system.

Appendix A. Supplementary data

Supplementary data to this article can be found online at https://doi.org/10.1016/j.redox.2022.102549.

References

[1] P.D. Ray, B.-W. Huang, Y.J.C.s. Tsuji, Reactive oxygen species (ROS) homeostasis and redox regulation in cellular signaling, 24, 2012, pp. 981–990, 5.
[2] D. Trachootham, J. Alexandre, P. Huang, Targeting cancer cells by ROS-mediated mechanisms: a radical therapeutic approach? Nat. Rev. Drug Discov. 8 (7) (2009) 579–591.
[3] K.K. Borowicz-Reutt, S.J. Czuczwar, Role of oxidative stress in epileptogenesis and potential implications for therapy, Pharmacol. Rep. 72 (5) (2020) 1218–1226.
[4] R. Zhang, et al., Nrf2—a promising therapeutic target for defensing against oxidative stress in stroke, Mol. Neurobiol. 54 (8) (2017) 6006–6017.
[5] J. Bhatti, et al., Systematic review of human and animal studies examining the efficacy and safety of N-acetylcysteine (NAC) and N-acetylcysteine amide (NACA) in traumatic brain injury: impact on neurofunctional outcome and biomarkers of oxidative stress and inflammation, Front. Neurol. 8 (2017) 744.
[6] J.N. Pearson-Smith, M. Patel, Metabolic dysfunction and oxidative stress in epilepsy, Int. J. Mol. Sci. 18 (11) (2017) 2365.
[7] X. Wang, et al., Oxidative stress and mitochondrial dysfunction in Alzheimer's disease, Biochim. Biophys. Acta (BBA) - Mol. Basis Dis. 1842 (8) (2014) 1240–1247.
[8] C. Cheignon, et al., Oxidative stress and the amyloid beta peptide in Alzheimer's disease, Redox Biol. 14 (2018) 450–464.
[9] L. Puspita, S.Y. Chung, J.-w. Shim, Oxidative stress and cellular pathologies in Parkinson's disease, Mol. Brain 10 (1) (2017) 1–12.
[10] R.R. Pestana, et al., Reactive oxygen species generated by NADPH oxidase are involved in neurodegeneration in the pilocarpine model of temporal lobe epilepsy, Neurosci. Lett. 484 (3) (2010) 187–191.
[11] S. Kovac, et al., Seizure activity results in calcium- and mitochondria-independent ROS production via NADPH and xanthine oxidase activation, Cell Death Dis. 5 (10) (2014), e1442.
[12] J.H. Kim, et al., Post-treatment of an NADPH oxidase inhibitor prevents seizure-induced neuronal death, Brain Res. 1499 (2013) 163–172.
[13] A.Y. Abramov, L. Canevari, M.R. Duchen, Beta-amyloid peptides induce mitochondrial dysfunction and oxidative stress in astrocytes and death of neurons through activation of NADPH oxidase, J. Neurosci. 24 (2) (2004) 565–575.
[14] A.Y. Abramov, A. Scorziello, M.R. Duchen, Three distinct mechanisms generate oxygen free radicals in neurons and contribute to cell death during anoxia and reoxygenation, J. Neurosci. 27 (5) (2007) 1129–1138.
[15] A. Saadi, et al., Spatial, temporal, and cell-type-specific expression of NADPH Oxidase isoforms following seizure models in rats, Free Radic. Biol. Med. 190 (2022) 158–168.
[16] S. Kaech, G. Banker, Culturing hippocampal neurons, Nat. Protoc. 1 (5) (2006) 2406–2415.
[17] S. Sandouka, T. Shekh-Ahmad, Induction of the Nrf2 pathway by sulforaphane is neuroprotective in a rat temporal lobe epilepsy model, Antioxidants 10 (11) (2021).
[18] T. Shekh-Ahmad, et al., Combination antioxidant therapy prevents epileptogenesis and modifies chronic epilepsy, Redox Biol. 26 (2019), 101278.
[19] T. Shekh-Ahmad, et al., Combination antioxidant therapy prevents epileptogenesis and modifies chronic epilepsy, Redox Biol. 26 (2019), 101278.
[20] T. Shekh-Ahmad, et al., KEAP1 inhibition is neuroprotective and suppresses the development of epilepsy, Brain 141 (5) (2018) 1390–1403.
[21] M.W. Pfaffl, A new mathematical model for relative quantification in real-time RT-PCR, Nucleic Acids Res. 29 (9) (2001), e45.
[22] M.A. Ansari, J.N. Keller, S.W. Scheff, Protective effect of Pycnogenol in human neuroblastoma SH-SY5Y cells following acrolein-induced cytotoxicity, Free Radic. Biol. Med. 45 (11) (2008) 1510–1519.
[23] J.L. Hellier, et al., Recurrent spontaneous motor seizures after repeated low-dose systemic treatment with kainate: assessment of a rat model of temporal lobe epilepsy, Epilepsy Res. 31 (1) (1998) 73–84.
[24] R.J. Racine, Modification of seizure activity by electrical stimulation. II. Motor seizure, Electroencephalogr. Clin. Neurophysiol. 32 (3) (1972) 281–294.
[25] Y. Ben-Ari, Limbic seizure and brain damage produced by kainic acid: mechanisms and relevance to human temporal lobe epilepsy, Neuroscience 14 (2) (1985) 375–403.
[26] G. Paxinos, C. Watson, The Rat Brain in Stereotaxic Coordinates: Hard Cover Edition, Elsevier, 2006.
[27] N. Pacico, A. Mingorance-Le Meur, New in vitro phenotypic assay for epilepsy: fluorescent measurement of synchronized neuronal calcium oscillations, PLoS One 9 (1) (2014), e84755.
[28] S. Kovac, et al., Prolonged seizure activity impairs mitochondrial bioenergetics and induces cell death, J. Cell Sci. 125 (7) (2012) 1796–1806.
[29] S. Schuchmann, et al., A relative energy failure is associated with low-Mg2+ but not with 4-aminopyridine induced seizure-like events in entorhinal cortex, J. Neurophysiol. 81 (1) (1999) 399–403.
[30] S. Williams, et al., Status epilepticus results in persistent overproduction of reactive oxygen species, inhibition of which is neuroprotective, Neuroscience 303 (2015) 160–165.
[31] K. Bedard, K.H. Krause, The NOX family of ROS-generating NADPH oxidases: physiology and pathophysiology, Physiol. Rev. 87 (1) (2007) 245–313.
[32] K. Dohi, et al., Gp91phox (NOX2) in classically activated microglia exacerbates traumatic brain injury, J. Neuroinflammation 7 (1) (2010) 1–11.
[33] L. Park, et al., Nox2-derived radicals contribute to neurovascular and behavioral dysfunction in mice overexpressing the amyloid precursor protein, Proc. Natl. Acad. Sci. USA 105 (4) (2008) 1347–1352.
[34] C. Kleinschnitz, et al., Post-stroke inhibition of induced NADPH oxidase type 4 prevents oxidative stress and neurodegeneration, PLoS Biol. 8 (9) (2010).
[35] H. Girouard, et al., NMDA receptor activation increases free radical production through nitric oxide and NOX2, J. Neurosci. 29 (8) (2009) 2545–2552.
[36] B.Y. Choi, et al., Prevention of traumatic brain injury-induced neuronal death by inhibition of NADPH oxidase activation, Brain Res. 1481 (2012) 49–58.
[37] A. Malkov, et al., Activation of nicotinamide adenine dinucleotide phosphate oxidase is the primary trigger of epileptic seizures in rodent models, Ann. Neurol. 85 (6) (2019) 907–920.
[38] W.Y. Huang, et al., NADPH oxidases as potential pharmacological targets against increased seizure susceptibility after systemic inflammation, J. Neuroinflammation 15 (1) (2018) 140.
[39] J. Wang, R.A. Swanson, Superoxide and non-ionotropic signaling in neuronal excitotoxicity, Front. Neurosci. 4 (2020) 861.
[40] A.M. Minnella, et al., Excitotoxic superoxide production and neuronal death require both ionotropic and non-ionotropic NMDA receptor signaling, Sci. Rep. 8 (1) (2018), 17522.
[41] F.E. Rey, et al., Novel competitive inhibitor of NAD(P)H oxidase assembly attenuates vascular O(2)(-) and systolic blood pressure in mice, Circ. Res. 89 (5) (2001) 408–414.
[42] M.E. Cifuentes-Pagano, D.N. Meijles, P.J. Pagano, Nox inhibitors & therapies: rational design of peptidic and small molecule inhibitors, Curr. Pharmaceut. Des. 21 (41) (2015) 6023–6035.
[43] G. Csányi, et al., Nox2 B-loop peptide, Nox2ds, specifically inhibits the NADPH oxidase Nox2, Free Radic. Biol. Med. 51 (6) (2011) 1116–1125.

[44] F. Rey, et al., Novel competitive inhibitor of NAD (P) H oxidase assembly attenuates vascular O2− and systolic blood pressure in mice, Circ. Res. 89 (5) (2001) 408–414.
[45] P. Sukumar, et al., Nox2 NADPH oxidase has a critical role in insulin resistance–related endothelial cell dysfunction, Diabetes 62 (6) (2013) 2130–2134.
[46] T. Ebrahimian, et al., Mitogen-activated protein kinase–activated protein kinase 2 in angiotensin ii–induced inflammation and hypertension: regulation of oxidative stress, Hypertension 57 (2) (2011) 245–254.
[47] L. Park, et al., Nox2-derived reactive oxygen species mediate neurovascular dysregulation in the aging mouse brain, J. Cerebr. Blood Flow Metabol. 27 (12) (2007) 1908–1918.
[48] Y. He, et al., Prolonged exposure of cortical neurons to oligomeric amyloid-β impairs NMDA receptor function via NADPH oxidase-mediated ROS production: protective effect of green tea (-)-epigallocatechin-3-gallate, ASN Neuro 3 (1) (2011), AN20100025.
[49] J. Liu, et al., NAD(P)H oxidase mediates angiotensin II-induced vascular macrophage infiltration and medial hypertrophy, Arterioscler. Thromb. Vasc. Biol. 23 (5) (2003) 776–782.
[50] G.M. Jacobson, et al., Novel NAD (P) H oxidase inhibitor suppresses angioplasty-induced superoxide and neointimal hyperplasia of rat carotid artery, Circ. Res. 92 (6) (2003) 637–643.
[51] M. Al-Shabrawey, et al., Inhibition of NAD (P) H oxidase activity blocks vascular endothelial growth factor overexpression and neovascularization during ischemic retinopathy, Am. J. Pathol. 167 (2) (2005) 599–607.
[52] N.H. Lopes, et al., Rac-dependent monocyte chemoattractant protein-1 production is induced by nutrient deprivation, Circ. Res. 91 (9) (2002) 798–805.
[53] Q. Zeng, et al., Endothelin-1 regulates cardiac L-type calcium channels via NAD (P) H oxidase-derived superoxide, J. Pharmacol. Exp. Therapeut. 326 (3) (2008) 732–738.
[54] R. Harfouche, et al., Roles of reactive oxygen species in angiopoietin-1/tie-2 receptor signaling, Faseb. J. 19 (12) (2005) 1728–1730.
[55] N.E. Hahn, et al., Early NADPH oxidase-2 activation is crucial in phenylephrine-induced hypertrophy of H9c2 cells, Cell. Signal. 26 (9) (2014) 1818–1824.
[56] N. Duerrschmidt, et al., NO-mediated regulation of NAD (P) H oxidase by laminar shear stress in human endothelial cells, J. Physiol. 576 (2) (2006) 557–567.
[57] F. Krötz, et al., NAD (P) H oxidase–dependent platelet superoxide anion release increases platelet recruitment, Blood J. Am. Soc. Hematol. 100 (3) (2002) 917–924.
[58] R.M. Touyz, et al., Expression of a functionally active gp91phox-containing neutrophil-type NAD (P) H oxidase in smooth muscle cells from human resistance arteries: regulation by angiotensin II, Circ. Res. 90 (11) (2002) 1205–1213.
[59] A. Espinosa, et al., Myotube depolarization generates reactive oxygen species through NAD (P) H oxidase; ROS-elicited Ca2+ stimulates ERK, CREB, early genes, J. Cell. Physiol. 209 (2) (2006) 379–388.
[60] D. Riquelme, et al., High-frequency field stimulation of primary neurons enhances ryanodine receptor-mediated Ca2+ release and generates hydrogen peroxide, which jointly stimulate NF-κB activity, Antioxidants Redox Signal. 14 (7) (2011) 1245–1259.
[61] X.-F. Zhang, P. Forscher, Rac1 modulates stimulus-evoked Ca2+ release in neuronal growth cones via parallel effects on microtubule/endoplasmic reticulum dynamics and reactive oxygen species production, Mol. Biol. Cell 20 (16) (2009) 3700–3712.
[62] M. Jin, et al., Ca2+-dependent regulation of rho GTPases triggers turning of nerve growth cones, J. Neurosci. 25 (9) (2005) 2338–2347.
[63] J.D. Lambeth, NOX enzymes and the biology of reactive oxygen, Nat. Rev. Immunol. 4 (3) (2004) 181–189.
[64] C. Wilson, et al., A feed-forward mechanism involving the NOX complex and RyR-mediated Ca2+ release during axonal specification, J. Neurosci. 36 (43) (2016) 11107–11119.
[65] C. Szabó, H. Ischiropoulos, R. Radi, Peroxynitrite: biochemistry, pathophysiology and development of therapeutics, Nat. Rev. Drug Discov. 6 (8) (2007) 662–680.
[66] G. Jaiswal, P. Kumar, Neuroprotective role of apocynin against pentylenetetrazole kindling epilepsy and associated comorbidities in mice by suppression of ROS/RNS, Behav. Brain Res. 419 (2022), 113699.
[67] S.H. Lee, et al., Inhibition of NADPH oxidase activation by apocynin rescues seizure-induced reduction of adult hippocampal neurogenesis, Int. J. Mol. Sci. 19 (10) (2018) 3087.
[68] D. Bertoglio, et al., Kainic acid-induced post-status epilepticus models of temporal lobe epilepsy with diverging seizure phenotype and neuropathology, Front. Neurol. 8 (2017) 588.
[69] B. Van Nieuwenhuyse, et al., The systemic kainic acid rat model of temporal lobe epilepsy: long-term EEG monitoring, Brain Res. 1627 (2015) 1–11.
[70] D.R. Hernandez-Espinosa, et al., Role of NADPH oxidase-2 in the progression of the inflammatory response secondary to striatum excitotoxic damage, J. Neuroinflammation 16 (1) (2019) 91.
[71] A. Vezzani, R. Dingledine, A.O. Rossetti, Immunity and inflammation in status epilepticus and its sequelae: possibilities for therapeutic application, Expert Rev. Neurother. 15 (9) (2015) 1081–1092.
[72] T. Fabisiak, M. Patel, Crosstalk between neuroinflammation and oxidative stress in epilepsy, Front. Cell Dev. Biol. 10 (2022), 976953.
[73] C. Almeida, et al., Distinct cell-specific roles of NOX2 and MyD88 in epileptogenesis, Front. Cell Dev. Biol. 10 (2022), 926776.
[74] P.B. McElroy, et al., Scavenging reactive oxygen species inhibits status epilepticus-induced neuroinflammation, Exp. Neurol. 298 (Pt A) (2017) 13–22.
[75] T. Shekh-Ahmad, et al., Reactive oxygen species in status epilepticus, Epilepsy Behav. 101 (2019), 106410.
[76] C.L. Eastman, R. D'Ambrosio, T. Ganesh, Modulating neuroinflammation and oxidative stress to prevent epilepsy and improve outcomes after traumatic brain injury, Neuropharmacology 172 (2020), 107907.
[77] A.M. Brennan, et al., NADPH oxidase is the primary source of superoxide induced by NMDA receptor activation, Nat. Neurosci. 12 (7) (2009) 857–863.
[78] O. Jung, et al., gp91phox-containing NADPH oxidase mediates endothelial dysfunction in renovascular hypertension, Circulation 109 (14) (2004) 1795–1801.
[79] J.Y. Kim, et al., NOX inhibitors - a promising avenue for ischemic stroke, Exp. Neurobiol. 26 (4) (2017) 195–205.